Molecular-Recognition-Directed Self-Assembly of Pleated Sheets from 2-Aminopyrimidine Hydrogen-Bonding Motifs

by **Michael J. Krische** and **Jean-Marie Lehn***

Laboratoire de Chimie Supramoléculaire, ESA 7006 of the CNRS, ISIS, Université Louis Pasteur, 4, rue Blaise Pascal, F-67000 Strasbourg

and **Nathalie Kyritsakas** and **Jean Fischer**

Laboratoire de Cristallochimie, UMR 75 of the CNRS, Institut Le Bel, Université Louis Pasteur, 4, rue Blaise Pascal, F-67000 Strasbourg

The self-assembly of the 2,2′-diamino-5,5′-(dialkylmethylidene)methylenedipyrimidine derivatives **3a**–**c** allows for the molecular-recognition-directed generation of pleated sheets as revealed by X-ray crystallographic analysis. The data provide insight into the interplay of the different structural and interactional features of the molecular components in the generation of the supramolecular assembly. The introduction of the adamantylidene group as in **3c** leads to the dominance of the H-bonding factor and the resulting formation of a regular, fully interconnected array of pleated sheet type. The results suggest further manipulation of the interplay of the different factors to induce the self-assembly of other supramolecular architectures.

1. Introduction. – The development of a useful paradigm for molecular-recognition-directed self-assembly not only requires the presence of programmed components, but also that the strength, synergism, and specificity of the collective interactions be sufficient to exclude undesired modes of assembly. Such synergy becomes especially important in the engineering of H-bonded molecular solids where crystal-packing forces may be of the same order of magnitude as the predesigned interactions of the component molecules. Indeed, the interplay of the many attractive and repulsive interactions in the solid state is sufficiently complex that *a priori* prediction of crystal-packing arrangements *via* computational methods is viable for only rather simple systems and remains a worthy endeavor [1]. Thus, in the design of programmed molecular components, one incorporates motifs of well-defined binding strength and directionality, whose geometric requirements are compatible, even synergistic, with the steric requirements of the object one desires to generate. For H-bonding systems, these guidelines have been implemented in our laboratories in the design of homo- and heteroleptic components for the formation of molecular ribbons [2], molecules that specifically recognize mismatched base pairs in DNA strands [3], polymeric liquid crystalline supramolecular materials [4], recognition units for the specific aggregation and fusion of vesicles [5], and templates for deconvolution/selection in dynamic combinatorial libraries [6].

Selective self-assembly to yield one of many possible noncovalent objects amounts to chemical programming and implies that the required information be stored in the molecular components and read-out in a specific manner following a well-defined interactional algorithm [7]. We have previously demonstrated such read-specificity *via*

chirality control in the self-assembly of chiral nonracemic *vs.* chiral racemic molecular components [8] and the spontaneous self-sorting of chiral molecular components from a racemic mixture [9]. Another means of affecting read-specificity involves the incorporation of structural features that become sterically repulsive upon formation of an alternative, undesired object or would yield arrangements in which the packing contribution is not maximized. Here, we describe a system in which the assembly process is influenced by these latter varieties of read-specificity.

2. Design Strategy. – As part of a general investigation of self-assembly in H-bonded systems [10], we were interested in constructing a two-dimensional H-bonded network, or β-network, reminiscent of the protein secondary-structure motif, the β-pleated sheet. Our interest was twofold. As nonlinear optical properties, ferromagnetic behavior, electrical conductivity, and solid-state reactivity all depend crucially on the relative orientation of the composite molecules in the solid state, a general strategy for the construction of surfaces possessing organized, periodic arrays of protruding functional substituents would be valuable from a material-science perspective. Of perhaps greater significance is the development of a general paradigm for the logic-driven retrosynthesis of molecular solids allowing for the rational design of their composite tectons.

Our design of a programmed molecular-component encoding for pleated sheet formation takes advantage of the known homomeric H-bonding motif expressed by 2-aminopyrimidines [10b], a recognition group of the '*Janus*' type presenting two self-complementary H-bonding interaction faces. In the solid state, 2-aminopyrimidines yield a one-dimensional object, a doubly H-bonded ribbon. Combining one-dimensional motifs *via* covalent attachment of two 2-aminopyrimidines in the 5,5′-positions should allow for propagation in a second dimension. A dialkylmethylidene substituent, at the bridge as in compound **3**, seemed ideally suited for such a scaffold, as it would enforce a cofacial arrangement of the bipyrimidines due to 1,3-allylic strain [11] and impart a fixed, relative geometrical orientation of *ca.* 120° (*Fig. 1*).

The optimal mode of self-assembly for **3** requires that each 2-aminopyrimidine be involved in the formation of a H-bonded ribbon. Interdigitation of alkylidene substituents may, in principle, occur along the axis parallel to the H-bonded ribbon and the axis orthogonal to the H-bonded ribbon resulting in the creation of hydrophilic and hydrophobic layers in the solid state. The presence of a 6.9-Å spacing between alternate pyrimidines of a given ribbon should allow for the interdigitation of sufficiently small alkylidene (especially aromatic) substituents along the axis parallel to the H-bonded ribbon. An alternative mode of self-assembly involves the formation of a cyclic hexamer defining a tube of *ca.* 15-Å diameter; however, such an arrangement does not permit maximization of the packing contribution (*Fig. 2*).

3. Synthesis of the Molecular Components. – For the synthesis of the molecular components, we searched for a highly convergent, modular sequence that would allow for the aquisition of a series of analogous compounds in preparative quantities. The synthesis of **3** involves double *Stille* coupling of the *N*-protected 5-(trialkylstannyl)-pyrimidine **1** with the geminal vinylic dibromide **2**. The viability of this approach hinged upon the success of this double *Stille* coupling which, to the best of our knowledge, is unprecedented (*Scheme 1*).

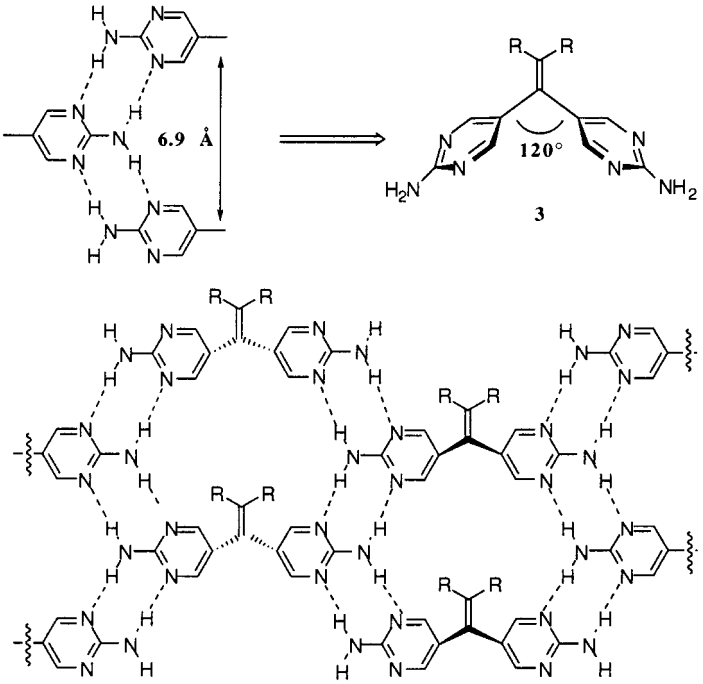

Fig. 1. *Design of a surface* via *combination of one-dimensional motifs*

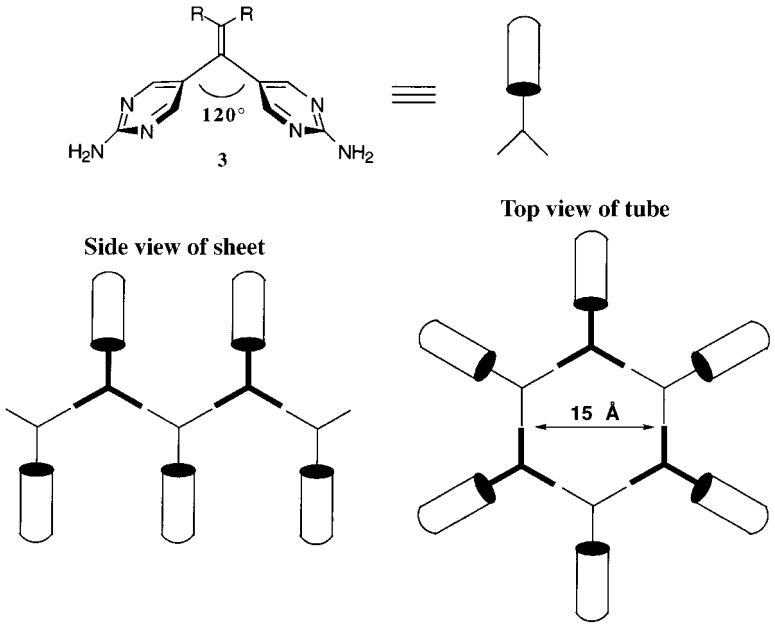

Fig. 2. *Possible modes of self-assembly: sheet* vs. *tube formation.* Left: *Side view of sheet;* right: *top view of tube.*

Scheme 1. *Strategy for the Synthesis of the Molecular Components*

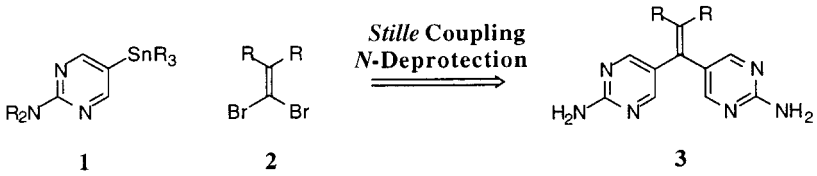

1 **2** **3**

The *N*-protected 5-(trialkylstannyl)pyrimidine **1** was prepared in a straightforward manner. Melting of commercially available 2-amino-5-bromopyrimidine with phthalic anhydride provided 5-bromo-2-phthalimidopyrimidine which smoothly underwent Pd-catalyzed stannylation utilizing hexamethylditin [12] to afford the requisite partner **1** for *Stille* coupling as a white powder (m.p. 178–179°). Double *Stille* cross-coupling of **1** with the known geminal vinylic dibromides **2a** [13], **2b** [14], and **2c** [15] employing tetrakis(triphenylphosphine)palladium(0) as catalyst was very sluggish giving only 5% of the bis-coupled product after three days. The use of tris(dibenzylideneacetone)di-palladium(0) in conjunction with tri(2-furyl)phoshine [16] led to a dramatic increase in the rate of reaction providing the *N*-protected bis-coupled products **3a**, **3b**, and **3c** in 72%, 99%, and 82% yields, respectively, after only 24 h. Cleavage of the protecting phthalimido group with methyl hydrazine then provided the components for self-assembly (*Scheme 2*).

Scheme 2. *Synthesis of the Molecular Components*

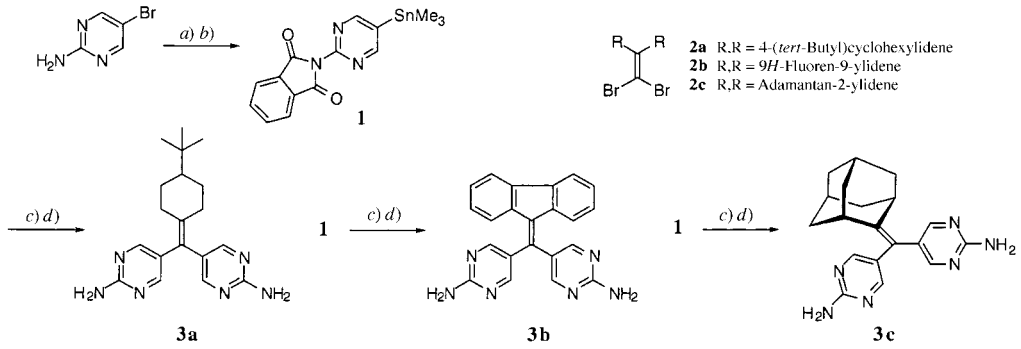

3a **3b** **3c**

a) Phthalic anhydride, 190°; 40–60%. *b*) $Pd(PPh_3)_4$, Sn_2Me_6, PhMe, 100°; 70%. *c*) $[Pd_2(dba)_3]\cdot CHCl_3$ **2a** or **2b**, $(2\text{-furyl})_3P$, PhMe, 100°; **3a**: 72%, **3b**: 99%, **3c**: 82%. *d*) $MeNHNH_2$, DCM, 25°; **3a**: 89%, **3b**: 93%, **3c**: 88%.

4. Self-Assembly in the Solid State: Structure Analysis. – The self-assembly of the self-complementary components **3a**, **3b**, and **3c** was studied in the solid state by determination of the corresponding crystal structures.

Tecton **3a** was crystallized by slow evaporation from an AcOEt solution. Its crystal structure was determined, revealing an interdigitated, H-bonded pleated sheet motif. Several other interesting aspects were evident. Unlike the model structure described in *Fig. 1*, for **3a** the alkylidene substituents of alternate dipyrimidines along the ribbon axis project in opposite directions. This deviation presumably arises in order to maximize packing. The 4-(*tert*-butyl)cyclohexylidene substituents are too large to permit

interdigitation along the ribbon axis, yet they are of insufficient size to fully occupy the 6.9-Å spacing between alternate dipyrimidines. The H-bonds alone are not strong enough to energetically compensate for the unoccupied space, and the observed structure is instead adopted. Since a coplanar disposition of alternating dipyrimidines is not evident, formation of all H-bonds is rendered geometrically unfeasible. This arrangement perturbs the length and symmetry of the H-bonds. The average length of an NH···N H-bond is 3.07 ± 0.11 Å and, *e.g.*, it is 3.10 Å in 2-amino-5-bromopyrimidine [17]. One may consider that there is no NH···N distance beyond 3.75 Å [18]. In **3a**, the NH···N H-bonds between the *Janus* faces of the pyrimidines are unsymmetrical, each face displaying one strong and one weak (3.546-Å length) or even unsatisfied (4.122-Å distance) H-bond (*Fig. 3*).

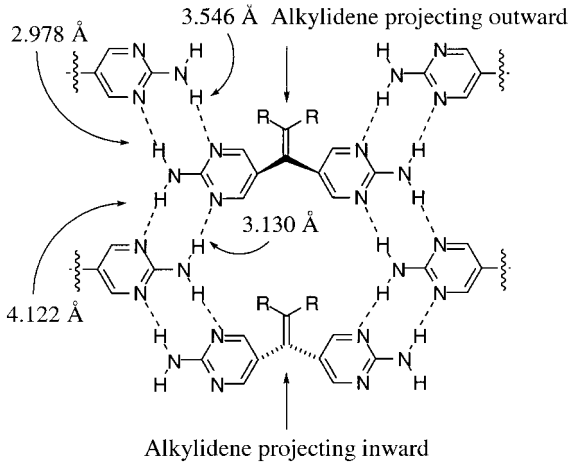

Fig. 3. *Alternating strong-weak H-bonds of the* Janus *faces of* **3a**

Segregated hydrophobic and hydrophilic layers involving interdigitation of the hydrophobic 4-(*tert*-butyl)cyclohexylidene moieties is clearly observed in a cross section of the surface (*Fig. 4*). Most interestingly, the hydrophilic regions of two independent surfaces were found to be interwoven [19]. A view along the plane of the surface, in which the 4-(*tert*-butyl)cyclohexylidene groups are omitted for clarity, reveals the interwoven pattern of H-bonding (*Fig. 5*). Finally, looking down upon the surface, one may observe interpenetration of the two independent two-dimensional networks (*Fig. 6*).

To promote generation of the desired β-network assembly, proper definition of the alkylidene substituent was required. We reasoned that a larger substituent, represented by the adamantan-2-ylidene **3c**, would address shortcomings present in the assembly of the cyclohexylidene derivative **3a**. The adamantanylidene moiety is sufficiently large to preclude interdigitation along the ribbon axis. Additionally, the secondary C-centers at the allylic positions of the adamantyl group should enforce the requisite co-facial orientation of the pyrimidines.

Upon cooling of a hot butanone solution of **3c**, crystals deposited. X-Ray crystallographic analysis indeed revealed a highly ordered pleated sheet in which all H-

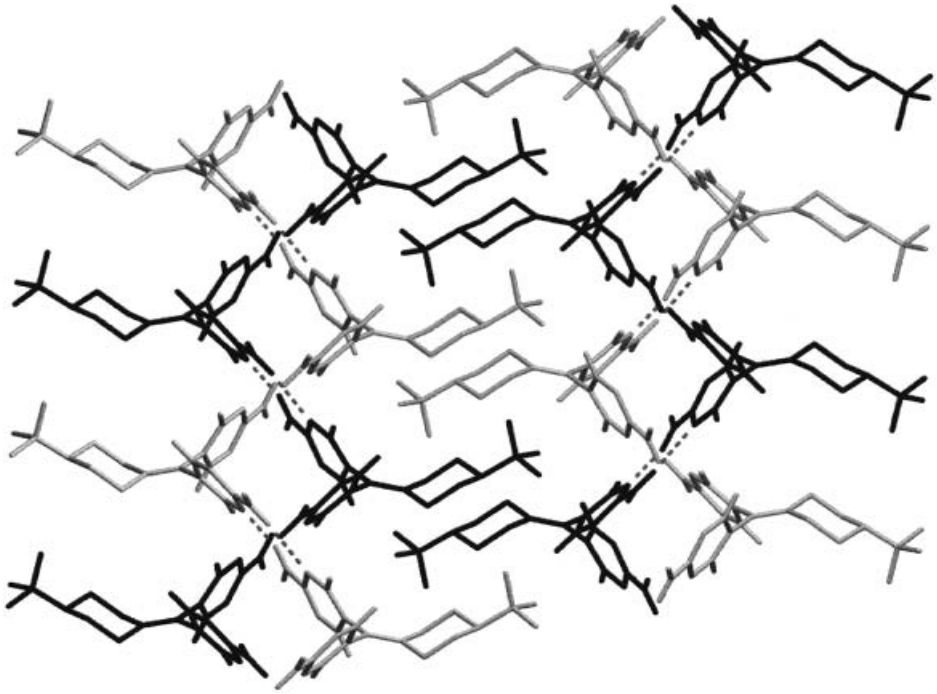

Fig. 4. *X-Ray structure of* **3a** *depicting interdigitation of the (*tert*-butyl)cyclohexylidene moieties and layering of the hydrophobic and hydrophilic regions*

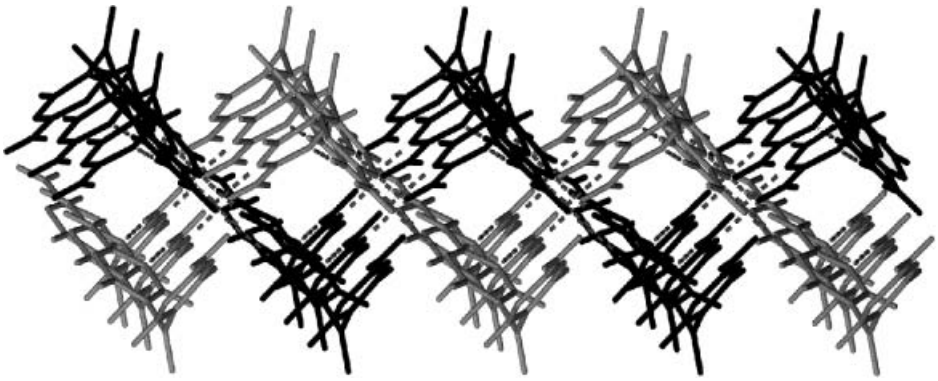

Fig. 5. *Interpenetration of two independent two-dimensional H-bonded networks in the X-ray crystal structure of* **3a** ((*tert*-butyl)cyclohexylidene groups omitted for clarity)

bonds are satisfied (NH···N lengths 3.024 and 3.045 Å) according to the model described in *Fig. 2*, and where the adamantylidene units alternate from one side of the sheet to the other. Viewing the surface from above shows the H-bonded ribbons (*Fig. 7*). Stacking of the surfaces is observed along the axis parallel to the H-bonded ribbons (*Fig. 8*). The adamantylidene group thus satisfies the requirements for driving

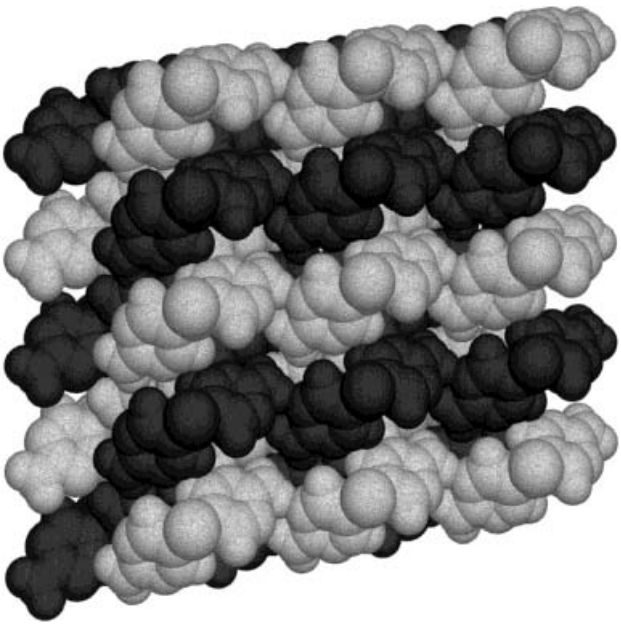

Fig. 6. *A top view of the interwoven β-networks in the X-ray crystal structure of* **3a** ((*tert*-butyl)cyclohexylidene groups omitted for clarity)

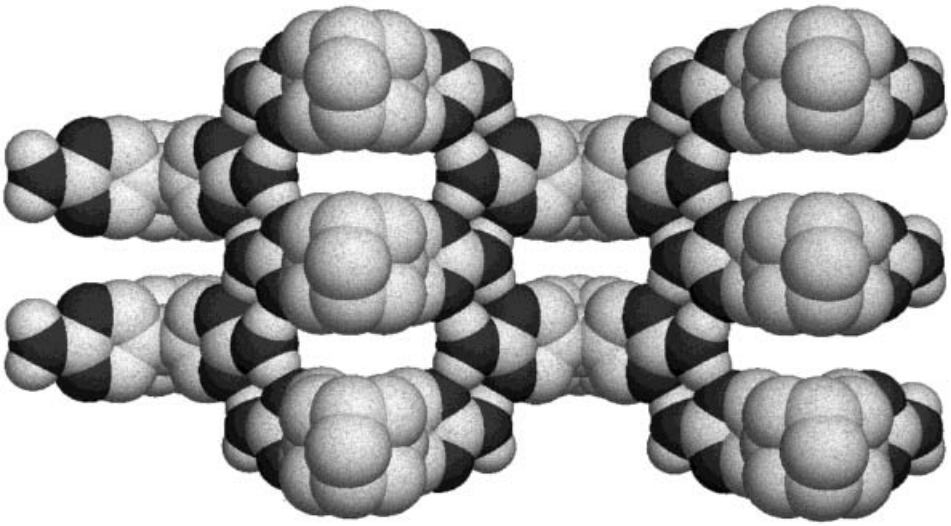

Fig. 7. *X-Ray crystal structure of* **3c** *view on the β-pleated sheet surface; space-filling representation* (solvent omitted for clarity)

the self-assembly towards the fully H-bonded two-dimensional pleated sheet supramolecular architecture, which is adopted by a number of synthetic peptides [20].

For self-assembly, to generate the desired object, synergy or at least a suitable balance between the supramolecular interactions is required. This is further illustrated

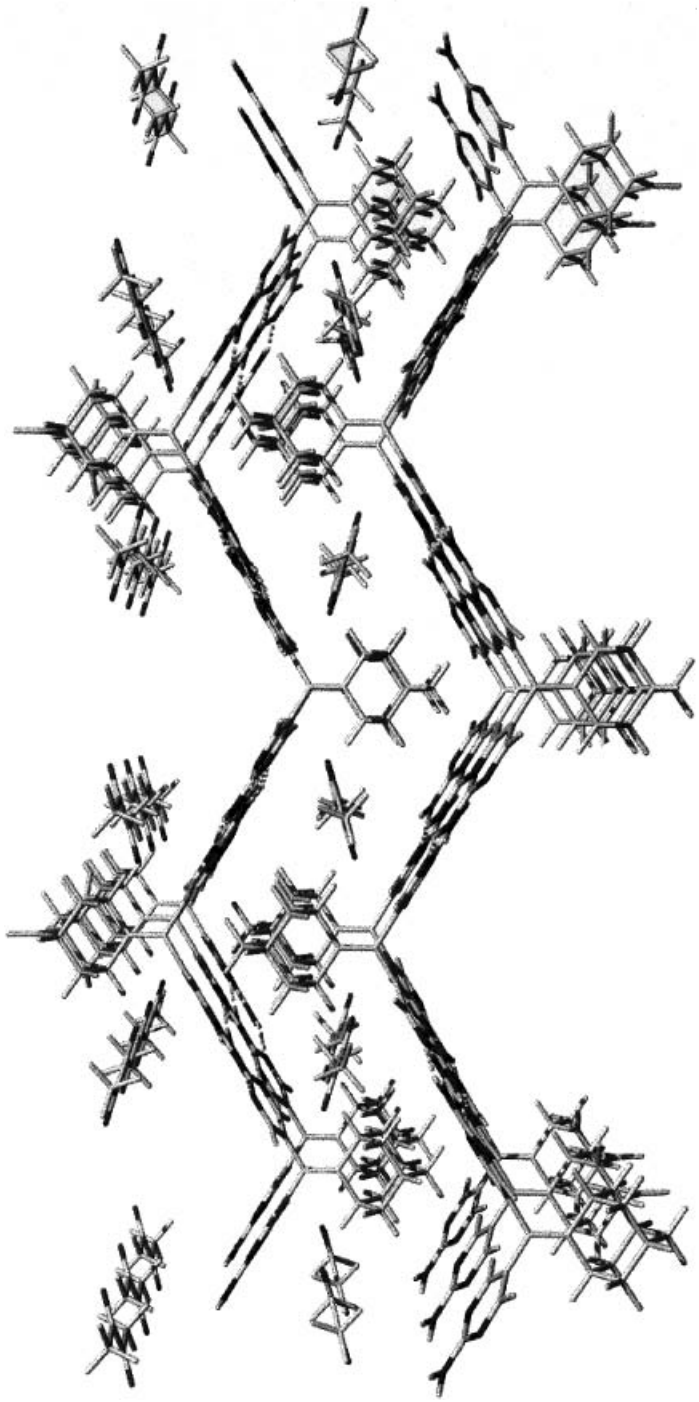

Fig. 8. *Stacking of the H-bonded surfaces in the crystal structure of* **3c**

in the X-ray crystal structure of the 9*H*-fluoren-9-ylidene derivative **3b** which gave identical crystalline polymorphs from AcOEt or PhCl (*Fig. 9*). A conflict arises here between the π-stacking and H-bonding contributions. If the arenes are to interdigitate, the derived H-bonded sheets must stack upon one another such that the pleats point in opposite directions, forming large gaps between layers. H-Bonding forces are unable to stabilize the porous structure for which the π-stacking interactions encode, and an assembly retaining half of the potential H-bonds results. The length is 3.056 Å for the H-bonds of the dimer and 3.048 Å for the single H-bond which deviates 65° from planarity (*Fig. 9*).

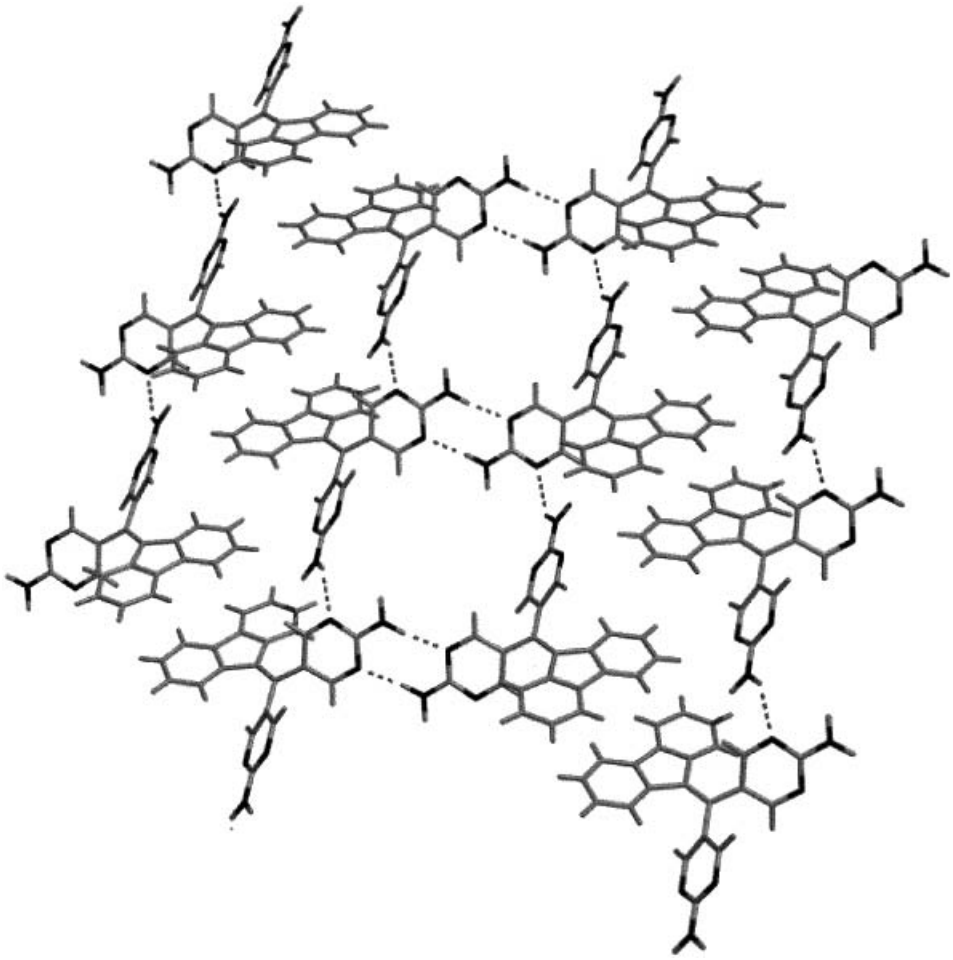

Fig. 9. *X-Ray crystal structure of* **3b** (ball-and-stick representation) *illustrating the H-bonding network and the stacking of the fluorenylidene groups*

The viability of molecular programming relies upon our capacity to identify and orchestrate the various supramolecular interactions such that all operate in consonance. In the specific case of H-bonded molecular solids, a suitable balance is required

between steric, *van der Waals*, π-stacking, and H-bonding information. Thus, the introduction of the adamantanylidene group in **3c** allows the H-bonding features of the 2-aminopyrimidine unit to play the dominant role, leading to a fully interconnected sheet where all binding capabilities are satisfied. Analysis of the data suggests further structural modification of the components to generate other types of supramolecular architectures, in particular, modifications allowing the passage from the sheet to the tube arrangement (*Fig. 2*), may be envisaged. The controlled engineering of molecular components bearing for instance electroactive, photoactive, or odd-electron residues may lead to functional self-organized materials endowed with novel electrical, optical, or magnetic properties.

We thank the *NIH* for a post-doctoral fellowship (*M.J.K.*), and *A. Krische* for her expert help in generating the figure graphics.

Experimental Part

General. Purchased reagents were used without purification. Toluene was distilled from Na metal under dry N_2. CH_2Cl_2 was distilled from CaH_2 under dry. N_2. M.p.: an electrothermal digital melting-point apparatus; uncorrected. IR Spectra: *Perkin-Elmer 1600* series *FTIR* instrument. ^{1}H-NMR Spectra: *Bruker SY 200* spectrometer, at 200 MHz. ^{13}C-NMR Spectra: *Bruker SY 200* or *Bruker ARX* 500-MHz spectrometer, at 50.3 and 125.72 MHz, respectively. Solvent was used as an internal reference for both ^{1}H- and ^{13}C-NMR spectra. EI- and FAB-MS: by the Service de Spectrometrie de Masse, Institut de Chimie, Université Louis Pasteur.

5-Bromo-2-phthalimido/pyrimidine. An intimate mixture of 2-amino-5-bromopyrimidine (5.0 g, 28.7 mmol, 100 mol-%) and phthalic anhydride (4.68 g, 31.6 mmol, 110 mol-%) was heated to 190° for 15 min under stirring. After cooling to r.t., the resultant tar was pulverized and extracted with boiling $CHCl_3$. The combined $CHCl_3$ extracts were filtered and evaporated onto silica. Chromatography (SiO_2; AcOEt/CH_2Cl_2 5:95) provided the title compound as a white powder in yields ranging from 40–60%. The product may be recrystallized from toluene. M.p. 144–145°. IR (film): 1759, 1726, 1542, 1423, 1378, 1081, 883, 781, 716. ^{1}H-NMR (200 MHz, (D_6)DMSO): 924 (*s*, 2 H); 8.00 (*m*, 4 H). ^{13}C-NMR (50.3 MHz, (D_6)DMSO): 165.0; 160.1; 151.0; 135.3; 130.7; 123.9; 119.4. EI-MS: Calc. for $C_{12}H_6BrN_3O_2$ (M^+): 302.9643; found: 302.9. Anal. calc.: C 47.40, H 1.99; found: C 47.64, H 2.02.

2-Phthalimido-5-(trimethylstannyl)pyrimidine (**1**). To a flask charged with 5-bromo-2-phthalimido/pyrimidine (2.5 g, 8.2 mmol, 100 mol-%) and Sn_2Me_6 (4.04 g, 12.3 mmol, 150 ml-%), toluene (41 ml, 0.2M) was added. Ar was bubbled through the suspension for *ca*. 5 min, then $Pd(PPh_3)_4$ (379 mg, 0.32 mmol, 4.0 mol-%) was added. Ar was bubbled through the suspension for 1 additional min, and the reaction vessel was placed in 100° oil bath and stirred for 24 h. Then the reaction mixture was evaporated onto silica and chromatographed (SiO_2; AcOEt/CH_2Cl_2 1:99 →3:97) to provide **1** (2.23 g, 70% yield). White powder. M.p. 178–179°. IR (film): 3023, 1786, 1759, 1724, 1600, 1542, 1466, 1421, 1375, 1353, 1096, 1082, 882, 765. ^{1}H-NMR (200 MHz, $CDCl_3$): 8.86 (*s*, 2 H); 7.93 (*dd*, J = 5.65, 3.08, 2 H); 7.76 (*dd*, J = 5.47, 3.19, 2 H); 0.39 (*s*, 9 H). ^{13}C-NMR (50.3 MHz, $CDCl_3$): 165.8; 164.7; 153.3; 134.6; 133.6; 131.5; 123.9; −9.5. EI-MS: Calc. for $C_{15}H_{15}N_3O_2Sn$ (M^+): 389.0186; found: 389.0. Anal. calc.: C 46.44, H 3.90; found: C 46.48, H 3.91.

2,2′-Diamino-5,5′-{[4-(tert-*butyl)cyclohexylidene]methylene}dipyrimidine* (**3a**). To a flask charged with **1** (1.40 g, 3.63 mmol, 225 mol-%), *1-*(tert-*butyl)-4-(dibromomethylidene)cyclohexane* (**2a**; 500 mg, 1.6 mmol, 100 ml-%), and tri(furan-2-yl)phosphine (60 mg, 0.25 mmol, 16 mol-%), toluene (16 ml, 0.1M) was added. Ar was bubbled through the suspension for *ca*. 5 min. Then $[Pd_2(dba)_3]\cdot CHCl_3$ (33 mg, 0.032 mmol, 2.0 mol-%) was added. Ar was bubbled through the suspension for 1 additional min, and the reaction vessel was placed in 100° oil bath and stirred for 24 h. Then, the mixture was allowed to cool and filtered. The solid was washed with toluene and Et_2O to provide the highly insoluble bis-phthalimide (695 mg, 72% yield) as a brown powder. The bis-phthalimide (325 mg, 0.54 mmol, 100 mol-%) was directly suspended in CH_2Cl_2 (54 ml, 0.01M), and $MeNHNH_2$ (0.231 ml, 4.3 mmol, 800 mol-5%) was added. After 2 h, the mixture became homogenous and was evaporated onto silica. Chromatography (SiO_2; EtOH/CH_2Cl_2 5:95 →30:70) afforded **3a** (162 mg, 89%) as a white powder which was recrystallized by slow evaporation from AcOEt. M.p. 235–236°. IR (film): 3200, 2900, 1614, 1537, 1470, 749. ^{1}H-NMR (200 MHz, (D_6)DMSO): 7.95 (*s*, 4 H); 6.62 (*s*, 4 H); 2.55 (br. *s*, 1 H); 1.91

(br. *m*, 4 H); 1.20 (br. *m*, 4 H); 0.84 (*s*, 9 H). ^{13}C-NMR (125.7 MHz, (D_6)DMSO): 161.9; 158.1; 140.8; 123.8; 122.3; 47.4; 32.1; 31.6; 28.7; 27.4. EI-MS: Calc. for $C_{19}H_{26}N_6$ (M^+): 338.2219; found: 338.4.

2,2′-Diamino-5,5′-[(fluoren-9-ylidene)methylene]dipyrimidine (**3b**) was prepared from **1** and **2b**, as described for **3a**. The bis-phthalimide was obtained in 99% yield. $MeNHNH_2$-Mediated deprotection gave **3b** in 93% yield as an orange solid which was recrystallized from PhCl or slow evaporation from AcOEt. M.p. 345–346°. ^{1}H-NMR (200 MHz, $CDCl_3$): 8.29 (*s*, 4 H); 7.72 (*d*, $J = 8.1$, 2 H); 7.31 (*ddd*, $J = 8.3, 5.8, 2.6$, 2 H); 7.05 (*m*, 4 H); 5.38 (*s*, 4 H). ^{13}C-NMR (125.7 MHz, (D_6)DMSO): 163.1; 159.6; 139.5; 138.0; 135.9; 131.9; 127.4; 126.5; 123.7; 123.2. IR (film): 3200, 1614, 1587, 1537, 1470, 727. EI-MS: Calc. for $C_{22}H_{16}N_6$ (M^+): 364.1436; found: 364.4.

2,2′-Diamino-5,5′-[(adamantan-2-ylidene)methylene]pyrimidine (**3c**) was prepared from **1** and **2c**, as described for **3a**. The bis-phthalimide was obtained in 82% yield. $MeNHNH_2$-Mediated deprotection gave **3c** in 88% yield as a white solid which was recrystallized from butan-2-one. M.p. 289–290°. IR (film): 3451, 2915, 1626, 1588, 1469, 738. ^{1}H-NMR (200 MHz, (D_6)DMSO): 7.95 (*s*, 4 H); 6.62 (*s*, 4 H); 2.66 (br. *s*, 2 H); 1.90 (br. *m*, 12 H). ^{13}C-NMR (125.7 MHz, (D_6)DMSO): 162.0; 157.7; 148.6; 123.6; 118.6; 38.8; 36.3; 34.1; 27.3. EI-MS: Calc. for $C_{19}H_{22}N_6$ (M^+): 334.1906; found: 334.4.

Crystal Data for **3a**: $C_{19}H_{26}N_6$, M_r 338.46, monoclinic, space group $P2_1/c$, $a = 6.1210(2)$, $b = 29.1710(7)$, $c = 10.6680(2)$ Å, $\beta = 97.427(9)°$, $V = 1888.9(2)$ Å^3, $Z = 4$, $\rho_{calc.} = 1.19$ gcm^{-3}, $\mu(MoK_\alpha) = 0.070$ mm^{-1}. Colorless crystal of dimensions $0.16 \times 0.12 \times 0.08$ mm^3. 16344 reflections collected, $2.5° < \theta < 29.54°$. 2366 independant reflections having $I > 3\sigma(I)$. No absorption corrections. 226 parameters. Final results: $R(F) = 0.050$, $Rw(F) = 0.076$, $GOF = 1.444$, maximum residual electronic density = 0.19 eÅ^{-3}.

Crystal Data for **3b**: $C_{22}H_{16}N_6$, M_r 364.41, triclinic, space group $P\bar{1}$, $a = 9.001(1)$, $b = 10.239(1)$, $c = 10.798(1)$, $\beta = 118.01(9)°$, $V = 874(1)$ Å^3, $Z = 2$, $\rho_{calc.} = 1.29$ gcm^{-3}, $\mu(MoK_\alpha) = 0.076$ mm^{-1}. Orange crystal of dimensions $0.15 \times 0.15 \times 0.10$ mm^3. A total of 7426 reflections, $2.5° < \theta < 26.37°$. 1825 reflections having $I > 3\sigma(I)$. No absorption corrections. Final results: $R(F) = 0.048$, $Rw(F) = 0.064$, $GOF = 1.243$, maximum residual electronic density = 0.21 eÅ^{-3}.

Crystal Data for **3c**: $C_{23}H_{30}N_6O$. M_r 406.54, orthorhombic, space group *Pnma* $a = 16.0685(5)$, $b = 18.3670(5)$, $c = 7.543(1)$, $V = 2226.2(4)$ Å^3, $Z = 4$, $\rho_{calc.} = 1.219$ gcm^{-3}, $\mu(MoK_\alpha) = 0.073$ mm^{-1}. Colorless crystal of dimensions $0.20 \times 0.15 \times 0.10$ mm^3. A total of 19686 reflections, $2.5° < \theta < 29.56°$. 1797 reflections having $I > 3\sigma(I)$. No absorption corrections. Final results: $R(F) = 0.066$, $Rw(F) = 0.080$, $GOF = 1.260$, maximum residual electronic density = 0.52 eÅ^{-3}.

In common: *Nonius KappaCCD* diffractometer, MoK_α graphite monochromated radiation ($\lambda = 0.71073$ Å), phi scans, 173 K. The structures were solved using direct methods and refined against $|F|$. H-Atoms were introduced as fixed contributors. For all computations, the *Enraf-Nonius* MolEN package was used (OpenMoleN, Interactive Structure Solution, Nonius B.V., Delft, The Netherlands, 1997). Further details of the crystal structure investigation are available on request from the Director of *Cambridge Crystallographic Data Centre*, 12 Union Road, Cambridge CB2 1EZ, UK, on quoting the full journal citation.

REFERENCES

[1] G. R. Desiraju, *Science* **1997**, *278*, 404; J. Perlstein, *J. Chem. Mater.* **1994**, *6*, 319; A. Gavezotti, *J. Am. Chem. Soc*. **1991**, *113*, 4622; A. Gavezotti, G. Filippini, *ibid*. **1996**, *118*, 7153; A. Gavezzotti, G. Fillipini, *J. Chem. Soc., Chem. Commun*. **1998**, 287; J. R. Holden, Z. Du, H. L. Ammon, *J. Comput. Chem.* **1993**, *14*, 422.

[2] J.-M. Lehn, M. Mascal, A. DeCian, J. Fischer, *J. Chem. Soc., Perkin Trans. 2* **1992**, 461; J.-M. Lehn, M. Mascal, A. DeCian, J. Fischer, *J. Chem. Soc., Chem. Commun*. **1990**, 479.

[3] N. Branda, G. Kurz, J.-M. Lehn, *J. Chem. Soc., Chem. Comm*. **1996**, 2443.

[4] C. Fouquey, J.-M. Lehn, A.-M. Levelut, *Adv. Mater.* **1990**, *2*, 254; T. Gulik-Krzywicki, C. Fouquey, J.-M. Lehn, *Proc. Natl. Acad. Sci. U.S.A*. **1993**, *90*, 163.

[5] V. Marchi-Artzner, L. Jullien, T. Gullik-Krzywicki, J.-M. Lehn, *J. Chem. Soc., Chem. Commun*. **1997**, 117.

[6] I. Huc, M. J. Krische, D. P. Funeriu, J.-M. Lehn, manuscript in preparation.

[7] J.-M. Lehn, 'Supramolecuar Chemistry – Concepts and Perspectives', VCH, Weinheim, 1995, Chapt. 9.

[8] M.-J. Brienne, J. Gabard, M. Leclercq, J.-M. Lehn, M. Cesario, C. Pascard, M. Chevé, G. Dutruc-Rosset, *Tetrahedron Lett*. **1994**, *35*, 8157.

[9] K. C. Russell, J.-M. Lehn, N. Kyritsakas, A. Decian, J. Fischer, *New J. Chem.* **1998**, 123.

[10] a) M. Etter, *Acc. Chem. Res.* **1990**, *23*, 120; D. S. Lawrence, T. Jiang, M. Levett, *Chem. Rev.* **1995**, *95, 2229;* V. A. Russel, M. D. Ward, *Chem. Mater.* **1996**, *8*, 1654; b) M. C. Etter, D. A. Adsmond, *J. Chem. Soc., Chem. Commun.* **1990**, 589.

[11] R. W. Hoffmann, *Chem. Rev.* **1989**, *89*, 1841.
[12] M. Benaglia, S. Toyota, C. R. Woods, J. S. Siegel, *Tetrahedron Lett*. **1997**, *38*, 4737.
[13] G. H. Posner, G. L. Loomis, H. S. Sawya, *Tetrahedron Lett*. **1975**, 1373.
[14] G. C. Paul, J. J. Gajewski, *Synthesis* **1997**, 524.
[15] G. A. Olah, A.-H. Wu, *Synthesis* **1990**, 885.
[16] V. Farina, B. Krishnan, *J. Am. Chem. Soc*. **1991**, *113*, 9585.
[17] H. L. L. Watton, J. N. Low, P. Tollin, A. R. Howie, *Acta Crystallogr., Sect. C* **1988**, *44*, 1857.
[18] S. N. Vinogradov, R. H. Linell, in ' Hydrogen Bonding', Van Nostrand Reinhold Company, New York 1971, Chapt. 7-2.
[19] S. R. Batten, R. Robson, *Angew. Chem., Int. Ed. Engl.* **1998**, *37*, 1460.
[20] S. Zhang, C. Lockshin, R. Cook, A. Rich, *Biopolymers* **1994**, *34*, 663; J. S. Nowick, E. M. Smith, M. Pairish, *Chem. Soc. Rev.* **1996**, 401; S. Krauthäuser, L. A. Christianson, D. R. Powell, S. H. Gellman, *J. Am. Chem. Soc*.**1997**, *119*, 11720.

Received August 17, 1998